Characterization of Recombinant Wild Type and Site-Directed Mutations of Apolipoprotein C-III: Lipid Binding, Displacement of ApoE, and Inhibition of Lipoprotein Lipase†

Haiqun Liu,‡ Philippa J. Talmud,‡ Laurence Lins,§ Robert Brasseur,|| Gunilla Olivecrona,# Frank Peelman,⊥ Joël Vandekerckhove,⊥ Maryvonne Rosseneu,⊥ and Christine Labeur*,⊥

Centre for Cardiovascular Genetics, Department of Medicine, Royal Free and University College, London Medical School, London, INSERM U410, Paris, France, Centre de Biologique Moléculaire Numérique, University of Gembloux, Belgium, Department of Medical Biosciences, Medical Biochemistry, Umeå University, Sweden, and Department of Biochemistry, Ghent University, Belgium

Received April 25, 2000; Revised Manuscript Received June 5, 2000

ABSTRACT: The physicochemical properties of recombinant wild type and three site-directed mutants of apolipoprotein C-III (apoC-III), designed by molecular modeling to alter specific amino acid residues implicated in lipid binding (L9T/T20L, F64A/W65A) or LPL inhibition (K21A), were compared. Relative lipid binding efficiencies to dimyristoylphosphatidylcholine (DMPC) were L9T/T20L > WT >K21A > F64A/W65A with an inverse correlation with size of the discoidal complexes formed. Physicochemical analysis (Trp fluorescence, circular dichroism, and GdnHCl denaturation) suggests that L9T/T20L forms tighter and more stable lipid complexes with phospholipids, while F64A/W65A associates less tightly. Lipid displacement properties were tested by gel-filtrating apoE:dipalmitoylphosphatidylcholine (DPPC) discoidal complexes mixed with the various apoC-III variants. All apoC-III proteins bound to the apoE:DPPC complexes; the amount of apoE displaced from the complex was dependent on the apoC-III lipid binding affinity. All apoC-III proteins inhibited LPL in the presence or absence of apoC-II, with F64A/W65A displaying the most inhibition, suggesting that apoC-III inhibition of LPL is independent of lipid binding and therefore of apoC-II displacement. Taken together. these data suggest that the hydrophobic residues F64 and W65 are crucial for the lipid binding properties of apoC-III and that redistribution of the N-terminal helix of apoC-III (L9T/T20L) enhances the stability of the lipid-bound protein, while LPL inhibition by apoC-III is likely to be due to protein:protein interactions.

Apolipoprotein C-III is a 79 amino acid glycoprotein synthesized in the intestine and liver as components of both very low-density lipoproteins (VLDL) and high-density lipoproteins (HDL). The strong positive correlation between plasma apoC-III[1] levels and plasma triglyceride levels (Tg) and postprandial clearance (*1*−*4*) strongly suggests that apoC-III plays a major role in Tg metabolism. The distribution of apoC-III between HDL particles and non-HDL particles is a strong predictor of coronary atherosclerosis (*5*), and it has been suggested that increased apoC-III levels lead to an accumulation of apoB-rich particles (LpB:C-III) and result in a shift in the apoC-III distribution between VLDL and HDL, which leads to the decreased clearance and thus higher levels of circulating Tg-rich particles (*6*).

The amphipathic helices in all apolipoproteins promote binding to the lipid interface but with varying affinity (*7*), and this might form the basis for the action of apoC-III, such that excess apoC-III might lead to the displacement of other apoproteins from the lipoproteins. It has been suggested that the ability of apoC-III to displace apoC-II from the lipoprotein particles would reduce apoC-II activation of LPL (*8*) and increased plasma levels of apoC-III present in hypertriglyceridemic individuals would alter the apoC-III:C-II ratio, reducing LPL activation. In vitro studies show that a 3-fold molar excess of apoC-III reduced LPL activity by 25% (*9*). It has also been proposed that apoC-III acts as a direct noncompetitive inhibitor of LPL and this would require the presence of an apoC-III binding site on LPL (*10*). Sparrow et al. showed that the inhibitory effect of apoC-III could be localized to the C-terminal domain between residues 41 and 79 (*11*). However McConathy et al., using synthetic peptides of apoC-III, concluded that the N-terminus was the primary domain modulating LPL activity (*12*). Thus, there is some discrepancy as to the mechanism of apoC-III inhibition of LPL and the domains responsible for this inhibition.

A second outcome of raised plasma apoC-III levels is the displacement of apoE from lipoprotein particles, thus reducing the apoE-mediated clearance of Tg-rich remnant lipoproteins. Elevated Tg in human *APOC3* transgenic mice reflects the increased number of VLDL particles in the

† This work was supported by Biomed2 Concerted Action Grant PL 963324. P.J.T. is funded by the British Heart Foundation (RG95007).

* Correspondence should be addressed to this author at the Department of Biochemistry, Ghent University, Hospitaalstraat 13, B 9000 Gent, Belgium. Tel: +32/9/264.92.75. Fax: +32/9/264.94.96. E-mail: christine.labeur@rug.ac.be.

‡ London Medical School.

§ INSERM U410.

|| University of Gembloux.

⊥ Ghent University.

Umeå University.

[1] Abbreviations: apo, apolipoprotein; BSA, bovine serum albumin; DMPC, dimyristoylphosphatidylcholine; DPPC, dipalmitoylphosphatidylcholine; CD, circular dichroism; GdnHCl, guanidine hydrochloride; LPL, lipoprotein lipase; Tg, triglyceride(s).

10.1021/bi0009441 CCC: $19.00
Published on Web 07/14/2000

circulation which contain more Tg and apoC-III and less apoE, thereby diminishing apoE-mediated lipoprotein uptake (*13*). ApoC-III overexpression also reduces VLDL glycosaminoglycan binding, decreasing lipolysis at the cell surface (*14*). The displacement of apoE by apoC-III has recently been confirmed in vitro, but this is modulated by the size of the lipoprotein particles, with displacement of apoE by apoC-III from small LDL particles being more efficient than from large VLDL particles (*15*).

Naturally occurring mutations in apolipoprotein genes, particularly in apoE, apoB, apoC-II, and apoA-I (*16, 17*), have provided insight into the structure/function relationship of these proteins; however, such mutations are rare in apoC-III. A deletion of the *APOA1-C3-A4* gene locus identified in one family was associated with increased conversion of VLDL to IDL and LDL (*18*). Only four rare structural variants of apoC-III have been identified, but not all of these show clear association between the mutation and altered lipoprotein metabolism. Carriers of the $Gln_{38}Lys$ mutation have mildly elevated plasma apoC-III and Tg levels, and this could reflect the additional charge that might enhance lipid binding and/or alter the effect on LPL (*19*). $Asp_{45}Asn$ (*20*) and $Lys_{58}Glu$ (*21*) mutations result in the change or loss of a charge, but $Asp_{45}Asn$ carriers have normal lipid levels with increased VLDL-apoC-III content while Lys_{58}-Glu is associated with 30−40% lower apoC-III levels and with reduced Glu_{58}-apoC-III on VLDL and HDL, resulting in enrichment of HDL with apoE creating atypically large HDL particles. The $Thr_{74}Ala$ variant, which disrupts glycosylation, is associated with a normal lipid profile, suggesting that glycosylation does not have a profound impact on apoC-III function (*22, 23*).

Despite the large body of literature characterizing the function of apoC-III, this topic still remains a subject of debate. To study this, we have expressed recombinant wild type and site-directed mutations of apoC-III and undertaken detailed physicochemical studies to clarify further the lipid binding properties, apoE displacement, and inhibition of LPL by apoC-III.

EXPERIMENTAL PROCEDURES

Materials. Dimyristoylphosphatidylcholine (DMPC), dipalmitoylphosphatidylcholine (DPPC), bovine serum albumin (BSA), bovine lipoprotein lipase (LPL), and ampicillin were obtained from Sigma (Irvine, U.K.). GdnHCl was the highest purity and obtained from C. Roth, GmbH, Karlsruhe, Germany. Unless specified, all other reagents are from Sigma (p.a. grade). Glycerol tri[9,10-^{3}H]oleate, dNTP, and low molecular weight markers were purchased from Amersham-Pharmacia, U.K. All the primers, W-1 detergent, and DNA Taq polymerase were obtained from Gibco BRL, Paisley, U.K. The *E. coli* strains B834 (DE3) and BL21 (DE3) and pET23b vector were provided by Novagen, Bioscience, Cambridge, U.K. QuikChange Site-Directed Mutagenesis Kit was made by Stratagene, La Jolla, CA. All the related products, competent cells, and enzymes involved in the mutagenesis reaction were also provided in the kit. ApoE used for the preparation of the DPPC complexes is recombinant apoE3 prepared as previously described (*24*).

Molecular Modeling of Wild-Type ApoC-III and Mutants. (A) Hydrophobic Cluster Analysis (HCA). This method is based on a 2D helical plot of a given sequence (*25*). The sequence is written on an α-helix-like cylinder that is cut parallel to the main axis and unrolled. The unfolding of this cylinder thus separates adjacent residues, and the plot is duplicated to restore all amino acids in the vicinity. The hydrophobic residues are circled and hatched, allowing the detection of hydrophobic clusters whose size, shape, and composition can be analyzed (*25*). Long horizontal clusters are indicative of helices, while short vertical or mosaic clusters indicate the presence of β strands or turns.

(B) 3D Construction of Peptides. 3D construction of the peptides was carried out as previously described (*26, 27*). The method accounts for the contribution of the lipid−water interface, the concomitant variation of the dielectric constant, and the transfer energy of atoms from a hydrophobic to a hydrophilic environment (*28*).

(C) Secondary Structure Prediction. The secondary structure prediction is carried out at the NPS@ (Network Protein Sequence Analysis) web site (http://pbil.ibcp.fr/cgi-bin/npsa_automat.pl?page=/NPSA/npsa_seccons.html). Different predictive methods are used to obtain the consensus prediction: SOPMA (*29*), PHD (*30, 31*), Predator (*32*), GORIV (*33*), DPM (*34*), DSC (*35*), and SIMPA96 (*36, 37*).

All calculations were performed on Pentium-Pro processors, using PC-TAMMO+ (Theoretical Analysis of Molecular Membrane Organization) and PC-PROT+ (Protein Plus analysis) softwares. Graphs were drawn with the WinMGM program (Ab Initio Technology, France).

Generation of pET23b/APOC3 Construct. The human *APOC3* cDNA (a kind gift from Dr. John Taylor, San Francisco, CA) in the pBSSK vector (Stratagene) was used as a template for the amplification of the *APOC3* gene by PCR. This was performed in a 50 μL reaction containing 50 ng of plasmid DNA pBSSK/*APOC3* as template, 250 ng of each primer, and 1 unit of DNA polymerase in a buffer recommended by the manufacturers including 0.2 mM each dNTP and 1.5 mM $MgCl_2$. Two primers, the 5′ forward primer with an internal *Nde*I (underlined) site (5′-GGGAATTCCATATGTCAGAGGCCGAGGAT-3′) and a 3′ reverse primer designed to append the sequence for a 3′ *Xho*I restriction site (underlined) (5′-GTGGTGCTCGAGGGCAGCCACGGCTGAAG-3′), were used for PCR, using the following conditions: the initial cycle of 94 °C, 5 min; 66 °C, 1 min; and 72 °C, 2 min was followed by 35 cycles of 94 °C, 30 s; 66 °C, 1 min; and 72 °C, 1 min. Reactions were performed in an automated Omigene PCR machine (Hybaid Ltd., Middlesex, U.K). The resulting 264 bp human *APOC3* fragment was digested with *Nde*I and *Xho*I, and subcloned into a similarly digested pET23b vector following standard methodology. The ligation mixtures were transformed into competent cells of the XL1Blue strain of *E. coli* (Promega, Southampton, U.K.), and the transformed cells were selected with ampicillin (75 μg/mL) on LB-agar plates. The entire *APOC3* cDNA sequence was sequenced in both directions, using an ABI 377 prism DNA sequencer (Perkin-Elmer).

Generation of ApoC-III Variants. All the *APOC3* variants were generated by using the QuikChange Site-Directed Mutagenesis Kit (Stratagene). In a 50 μL reaction, 50 ng of plasmid DNA pET23b/*APOC3* was used as a template, and two synthetic oligonucleotide primers that contained the

Table 1: Primers Used To Generate the ApoC-III Variants by the in Vitro Mutagenesis Reactions

5′K21A	5′-CATGAAGCACGCCACCGCGACCGCCAAGGATGCAC-3′
3′K21A	5′-GTGCATCCTTGGCGGTCGCGGTGGCGTGCTTCATG-3′
5′F64AW65A	5′-AAGTTCTCTGAGGCCGCGGATTTGGACCC-3′
3′F64AW65A	5′-GGGTCCAAATCCGCGGCCTCAGAGAACTT-3′
5′L9T	5′-AGGATGCCTCCCTTACCAGCTTCATGCAGGG-3′
3′L9T	5′-CCCTGCATGAAGCTGGTAAGGGAGGCATCCT-3′
5′T20L	5′-GCTACATGAAGCACGCCCTCAAGCCGCCAAGGATG-3′
3′T20L	5′-CATCCTTGGCGGTCTTGAGGGCGTGCTTCATGTAGC-3′

desired mutation (underlined) and were complementary to the opposite strands of the vector were extended using Pfu Turbo DNA polymerase. *APOC3*-K21A was generated using primers 5′-K21A and 3′-K21A while *APOC3*-F64A/W65A was generated using primers 5′-F64A/W65A and 3′-F64AW65A. *APOC3*-L9T/T20L was generated by a two-step mutagenesis reaction, first by introducing the L9 to T9 substitution using primers 5′-L9T and 3′-L9T, and the resulting construct was used as a template to perform the second mutagenesis reaction using 5′-T20L and 3′-T20L, resulting in variant *APOC3*-L9T/T20L. All the primers used are listed in Table 1.

Expression and Purification of the Recombinant ApoC-III Variants. Plasmid DNA of pET23b/wild type-*APOC3* was transformed into competent *E. coli* B834 cells, and all the other *APOC3* variants in pET23b were transformed into *E. coli* BL21 respectively for optimum expression and used to inoculate an overnight culture in SOC medium containing 75 μg/mL ampicillin. Thirty milliliters of the overnight culture was used to inoculate 1 L of SOC medium (75 μg/mL ampicillin) and shaken (220 rpm/min) at 37 °C. Cells were induced with 0.5 mM IPTG until the OD_{600} of the cell culture reached 0.6, and were harvested by centrifugation at 3000 rpm (4 °C). The cells were lysed in 15 mL of 8 M urea, 50 mM NaH_2PO_4, 10 mM Tris-HCl, 500 mM NaCl (pH 8.0) buffer (by sonication on ice for 3 × 1 min) and then centrifuged at 18 000 rpm (30 min at 4 °C), and the supernatant was incubated with 1 mL of Talon cobalt metal affinity resin (Clontech, Hampshire, U.K.) for 2 h at 4 °C. The resin was pelleted by centrifugation (3000 rpm for 5 min), and batch-washed 4 times. The recombinant human apoC-III fusion proteins were eluted from the resin with 8 M urea, 50 mM NaH_2PO_4, 20 mM PIPES, and 500 mM NaCl (pH 6.0−6.3) buffer. The fractions containing recombinant apoC-III fusion protein were identified by electrophoresis on Tricine−SDS−PAGE (17.5% precast gels) (Bio-Rad, Hertfordshire, U.K.), and dialyzed overnight at 4 °C against 4 M urea, 5 mM NH_4HCO_3 (pH 8.0). This solution was loaded on an anion exchange Mono Q column (Pharmacia, Uppsala, Sweden) and eluted with a linear NaCl gradient (from 0.10 to 0.25 M) in 4 M urea, 5 mM NH_4HCO_3 (pH 8.0) buffer. The fractions containing the pure apoC-III protein (eluting at ±0.15 M NaCl) were pooled, and the final purity of the product was verified by Tricine−SDS−PAGE as described above. All the apoC-III variants were at least 95% pure. The protein content in the samples was determined by OD measurement at 280 nm using a molar extinction coefficient for apoC-III of 19 630 $M^{-1}\cdot cm^{-1}$.

Lipid Binding Properties of ApoC-III Variants. Association of recombinant apoC-III variants with lipid was followed by monitoring the turbidity decrease of dimyristoylphosphatidylcholine (DMPC) multilamellar vesicles at 325 nm as a function of the temperature. The DMPC vesicles were obtained as previously described (*38*), and 40 μg of apoC-III protein was added to 80 μg of DMPC vesicles in a 10 mM Tris-HCl, 150 mM NaCl buffer, pH 8.0, containing 8.5% KBr, 0.01% NaN_3, and 0.01% EDTA, in an Uvikon 931 spectrophotometer.

Preparation and Isolation of Phospholipid:ApoC-III Complexes. ApoC-III:DMPC complexes were prepared by incubation of the recombinant apoC-III proteins with DMPC multilamellar vesicles, at DMPC:protein (w/w) ratios of 2:1 at 25 °C for 16 h. The complexes were isolated by gel filtration on a Superose 6HR column (Pharmacia) in 10 mM Tris-HCl, 150 mM NaCl buffer, pH 7.6, and 0.2 g/L NaN_3 in an FPLC system (Waters). Complexes were detected by measuring the absorbance at 280 nm and the tryptophan (Trp) fluorescence emission at 330 nm (excitation at 295 nm). The Superose 6HR column was calibrated with a set of protein standards ranging from thyroglobulin (molecular mass 668 kDa) to cytochrome *c* (molecular mass 65 kDa) (Pharmacia). The resulting calibration curve was used for the determination of the molecular mass or Stokes radii of the particles eluting from the column.

Fluorescence Measurements. The maximum emission wavelength of the Trp fluorescence measurement was performed on an Aminco Bowman Series 2 spectrofluorometer (*39*). The lipid-free apoC-III protein at a protein concentration of 25 μg/mL and apoC-III:DMPC complexes at a protein concentration of 60 μg/mL were measured at room temperature. Emission spectra were recorded between 300 and 450 nm, with the excitation wavelength set at 295 nm.

Circular Dichroism Measurements. Circular dichroism (CD) spectra of each recombinant apoC-III protein in the presence or in the absence of 2,2,2-trifluoroethanol (TFE) were measured on a Jasco 600 spectropolarimeter at room temperature. Measurements were carried out at a protein concentration of 0.2 mg/mL in 10 mM Na_2HPO_4/NaH_2PO_4 buffer, pH 7.5. Nine spectra were collected and averaged for each sample. For the protein and protein/TFE mixtures, the secondary structures were obtained by curve-fitting on the entire ellipticity curve between 184 and 260 nm, using the software available on the Internet (http://bioinformatik.biochemtech.ini-halle.de/cdnn/).

For the denaturation experiments, the lipid-free apoC-III proteins and apoC-III:DMPC complexes, at a protein concentration of 100 μg/mL, were incubated for 12 h at 4 °C in the presence of increasing GdnHCl concentrations between 0 and 6 M prior to the CD measurements. The signal measured at 222 nm and expressed as molar ellipticity is plotted as a function of the GdnHCl concentration (M) in the sample.

Displacement of ApoE from ApoE:DPPC Complexes by ApoC-III Variants. The apoE:DPPC complexes were prepared by the sodium cholate dialysis method as described

(*40*) using DPPC at a ratio (w:w) of 2:1 and using recombinant apoE3 purified from *E. coli* as previously described (*24*). The protein−lipid mixtures were incubated overnight at 43 °C and then extensively dialyzed against 10 mM Tris-HCl buffer, pH 8, containing 150 mM NaCl and 0.1 g/L Na_2-EDTA and 1 mM azide, each time during 24 h at 43 °C, at room temperature, and at 4 °C. The homogeneity of the apoE:DPPC complexes was verified by gel filtration on a Superose 6 PG column where the complexes eluted in one homogeneous peak. The protein concentration in the complexes was determined by optical density measurement at 280 nm, and the phospholipid concentration was determined enzymatically (Biomérieux, Marcy l'Etoile, France). The concentrations of the complexes are expressed by their protein mass in all the following experiments. ApoE:DPPC complexes were mixed with the apoC-III proteins at a ratio of 1:1 (w:w) and incubated at room temperature for 3 h. The apoE:DPPC−apoC-III mixture was then separated by gel filtration on a Superose 6 PG column. The protein elution profile was recorded by measuring the Trp emission at 330 nm in each fraction. The content of apoE and apoC-III was measured in each fraction by sandwich ELISA as described (*41*). Briefly, antibodies were coated onto 96-well ELISA plates; residual binding sites were blocked, and samples or standards were incubated on the plates for 24 h, 37 °C. After excess antigen was washed away, the peroxidase-labeled antibody was incubated for 2 h at 37 °C. After washing, the amount of bound peroxidase was revealed with a chromogenic substrate. The plates were read, and the standard curve and samples were calculated with the software provided with the reader (Biotek, KC4 software). The sensitivity of the assays was approximately 2 ng.

Detection of ApoC-III and ApoE Proteins by Western Blotting. Samples were separated on Tricine−SDS−PAGE (17.5%), or on 15% SDS−PAGE. Proteins were transferred using a wet blot system (Bio-Rad) in a Tris (5 mM)−glycine (192 mM) buffer (pH 8.3) containing 20% methanol. Proteins were visualized with a rabbit anti-apoC-III antibody or a rabbit anti-apoE polyclonal antibody and a secondary peroxidase labeled goat anti-rabbit antibody. The bound peroxidase was visualized using the CN-DAB-kit (Pierce).

LPL Inhibition by ApoC-III Variants. Bovine LPL (EC 3.1.1.34) (Sigma, Irvine, U.K.) catalytic activity, in the presence of apoC-III variants, was measured using the emulsion Intralipid (Pharmacia Laboratories, Milton Keynes, U.K.) (100 mg/mL) into which [^{3}H]triolein had been incorporated by sonication (*42*). The incubation media contained 2% (v/v) of the emulsion, 6% (w/v) BSA (Sigma, Irvine, U.K.), 1.2% NaCl (w/v), 6.3% Tris-HCl (w/v), pH 8.5, and 3 IU of heparin (Sigma, Irvine, U.K.). As a source of apoC-II, human plasma apoC-II (*43*) was dissolved in 5 M urea, 10 mM Tris-HCl, pH 8.5, at 2 mg/mL. The experiments were optimized for both apoC-II and LPL, to give optimum hydrolysis with minimum apoC-II concentration. The emulsion was preincubated with each apoC-III sample with or without 2 μL of the 1:100 dilution of above apoC-II sample for at least 15 min; then the bovine LPL (10 μL of 1.5 μg/mL) was added in a final volume of 200 μL. The mixture was shaken in a water bath at 25 °C for 30 min. The reaction was stopped by extracting the fatty acids, and the radioactivity was counted (*42*).

RESULTS

Molecular Modeling of ApoC-III Variants. To obtain a better understanding of the structure/function relationship of apoC-III, molecular modeling was carried out. Consensus secondary structure prediction suggests that apoC-III is made of two helical domains: one in the N-terminal part, from approximately residues 5 to 40, and a second C-terminal helical domain localized at residues 45−60 (Figure 1A). Hydrophobic cluster analysis (HCA, explained under Experimental Procedures) of the entire apoC-III sequence identified two hydrophobic clusters at residues 6−20 and 42−66 localized within the two helical domains as detected from the secondary structure predictions analysis (Figure 1B). The shape and hydrophobic repartition in these clusters indicate that they are amphipathic helices, suggesting a potential role in lipid binding.

The 6−20 and 42−66 peptides were constructed in a 3D model, and their favored orientation at the lipid/water interface (Figure 2A,C) was calculated according to the method described (*28*). While the 42−66 peptide is clearly amphipathic, with its main axis mostly parallel to the interface (Figure 2C), the N-terminal peptide was tilted toward the interface, due to an uneven segregation of the hydrophilic and hydrophobic residues along the long axis of this particular α-helix (Figure 2C). Another interesting feature of the 42−66 helix was the unusually high content of aromatic residues (Phe, Trp, and to a lesser extent Tyr), especially at the C-terminus of the peptide.

To investigate the respective role of the N- and C-terminal domains of apoC-III, we designed mutants by modifying the amphipathicity and the aromatic content. The mutation in the N-terminal segment was obtained by permutation of the Leu9−Thr20 residues. This permutation avoided changes in hydrophobicity (that could have an effect by itself on the lipid binding properties) and restored amphipathicity, since its mean axis was oriented mostly parallel to the interface (Figure 2B). For the mutation in the C-terminus, Phe64 and Trp65 were mutated to Ala. These mutations changed the amphipathicity and the aromatic content (Figure 2D), as compared to the 42−66 wild-type apoC-III fragment (Figure 2C).

Expression and Purification of Recombinant ApoC-III Variants. To obtain large quantities of apoC-III proteins to investigate the structure−function relationship, an *E. coli* expression system was developed that yielded milligram quantities of the recombinant C-terminus His-tagged apoC-III proteins. For optimal expression, wild-type apoC-III was expressed in *E. coli* B834 while all other apoC-III mutants were expressed in *E. coli* BL21. After induction by IPTG at 37 °C, the fusion proteins reached about 5% of the total cellular protein. Since the fusion proteins were contained in inclusion bodies, they were purified in the presence of urea, using a combination of Talon affinity agarose and anion exchange chromatography. The resulting apoC-III fusion proteins were shown to be more than 95% pure (data not shown), and approximately 2 mg of the pure recombinant fusion protein was obtained from 1 L of culture medium.

Lipid Binding Properties of the ApoC-III Variants. DMPC binding experiments were performed to assess the interaction of the apoC-III variants with DMPC multilamellar vesicles. A scan through the transition temperature of DMPC (Figure

A

```
          10        20        30        40        50        60        70
          |         |         |         |         |         |         |
          |
apoc3wt
SEAEDASLLSFMQGYMKHATKTAKDALSSVQESQVAQQARGWVTDGFSSLKDYWSTVKDKFSEFWDLDPE
DPM
cchhhhhheeeehcehhhhhhhhhhhheeehhhhehhhhhceeeccccchtceeeeehthhhhhhchcch
DSC
ccchhhhhhhhhhhhhhhhhhhhhhhhhhhhhhhhhhhhhhhhhhcchhhhhhhhhcccccccchhccccc
GOR4
ccccccchhhhhhhhhhhhhhhhhhhhhhhhhhhhhhhhhhhhcccceeccccccccccccccccccccccccc
HNNC
ccchhhhhhhhhhhhhhhhhhhhhhhhhhhhhhhhhhhhhhhhhhhcchhhhhhhhhhhhhhhhhhccccccc
PHD
ccccchhhhhhhhhhhhhhhhhhhhhhhhhhhhhhhhhhhhhhhhhhhhhhhhhhhhhhhhhhhhhcccccccccc
Predator
ccchhhhhhhhhhhhhchhhhhhhhhhhhhhhhhhhhhhhcccccccccccccccccccccccccccccccccc
SIMPA96
cchhhhhhhhhhhhhhhhhhhhhhhhhhhhhhhhhhhhhhhhhhhcccccchhhhhhhhhhhhhhhhhhccccc
SOPMA
hhhhhhhhhhhhhhhhhhhhhhhhhhhhhhhhhhhhhhhhhhhtcchhhhhhhhhhhhhhhhhhhteeeccccc
Sec.Cons.
ccchhhhhhhhhhhhhhhhhhhhhhhhhhhhhhhhhhhhhhhcchhcc?hhhhhhhhhhhhhhcchccccccc
```

```
apoc3wt    VRPTSAVAA
DPM        eccccheccc
DSC        ccccccccc
GOR4       ccccceeec
HNNC       ccccccccc
PHD        ccccccccc
Predator   ccccccccc
SIMPA96    cccccceec
SOPMA      ccccchhhh
Sec.Cons.  ccccccccc
```

B

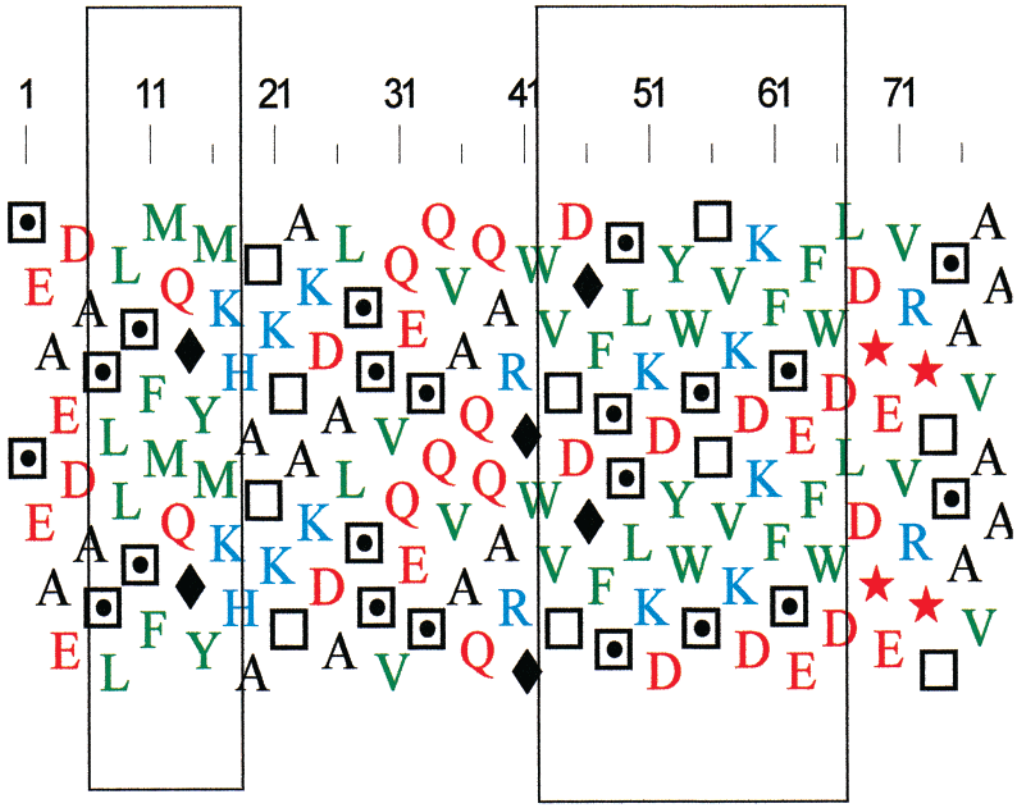

FIGURE 1: Sequence analysis of the apoC-III sequence. (A) Secondary structure prediction of apoC-III. Different predictive methods were used (see Experimental Procedures), and a consensus was obtained. Abbreviations: h, α-helix; e, β-sheet; c, coil; t, turn. (B) HCA plot of the apoC-III sequence. Hydrophobic residues (F, Y, W, M, L, I, V) are circled and hatched, red stars are Pro, black diamonds are Gly, white boxes are Thr, and pointed boxes are Ser. Negatively charged residues are red, and positively charged ones are blue. The two boxes indicate the main hydrophobic clusters of apoC-III.

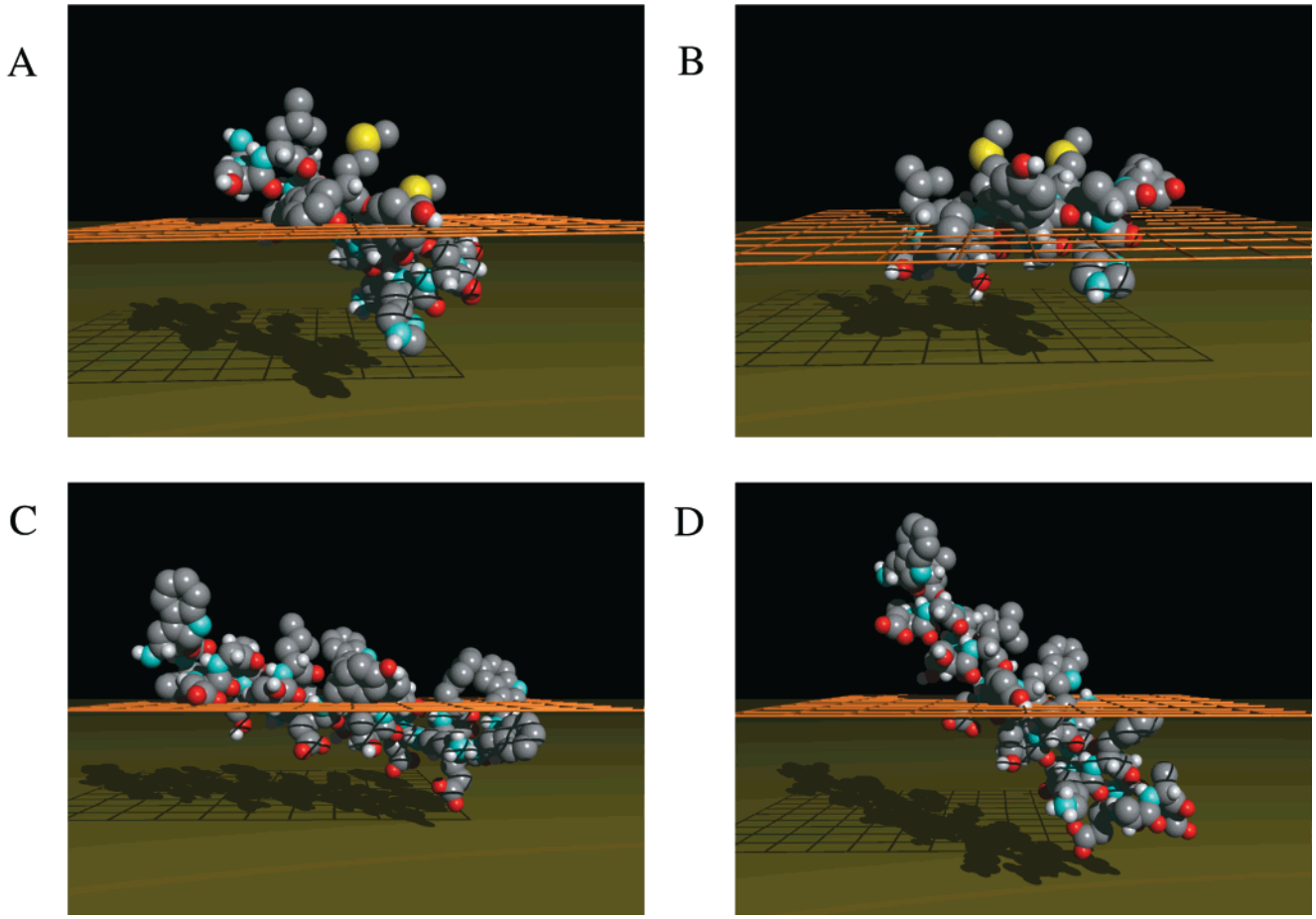

FIGURE 2: Orientation of the different apoC-III peptides (represented in CPK) at the lipid/water interface (orange plane). Lipid phase is above and water is below. (A) 6−20 peptide; (B) apoC-III-L9T/T20L mutant; (C) 42−66 peptide; (D) apoC-III-F64A/W65A mutant.

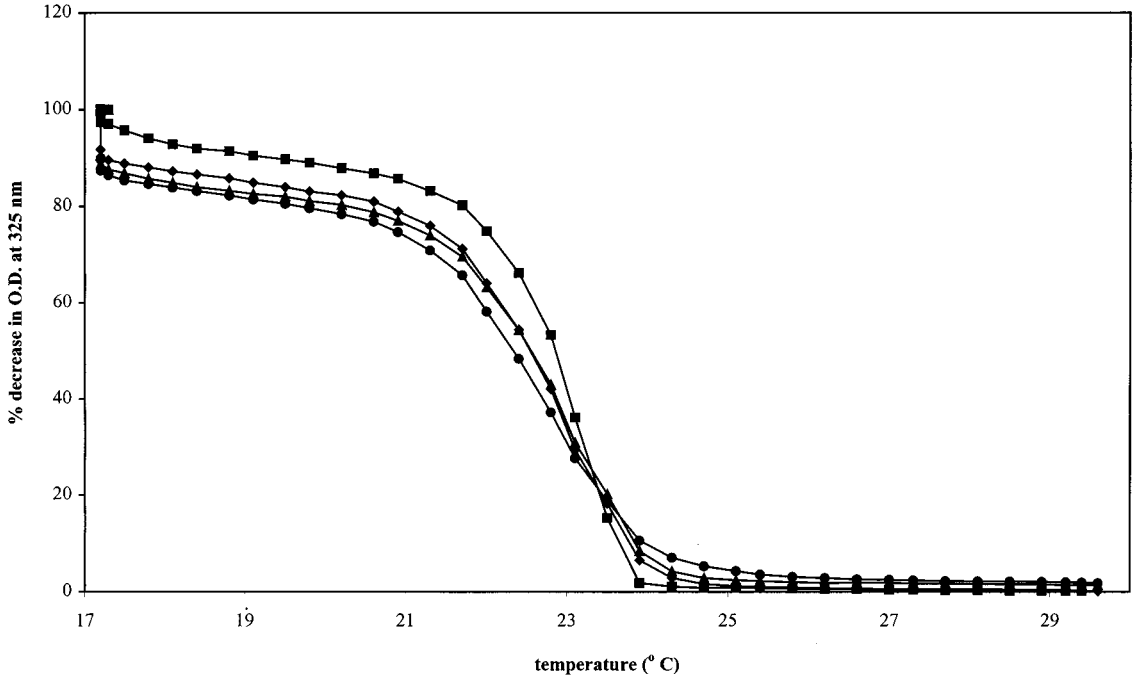

FIGURE 3: Turbidity decrease of DMPC multilamellar vesicles mixed with apoC-III at a w:w lipid:protein ratio of 2:1 expressed as a percentage decrease of the initial OD value at 325 nm as a function of temperature. (◆) WT apoC-III; (▲) apoC-III-K21A; (■) apoC-III-F64A/W65A; (●) apoC-III-L9T/T20L.

3) showed a turbidity decrease due to the formation of discoidal complexes. With all apoC-III proteins a similar decrease in the turbidity of the DMPC solution was observed that was maximal around the transition temperature of the DMPC. The resulting apoC-III:DMPC discoidal complexes were fractionated on a Superose 6 PG gel filtration column

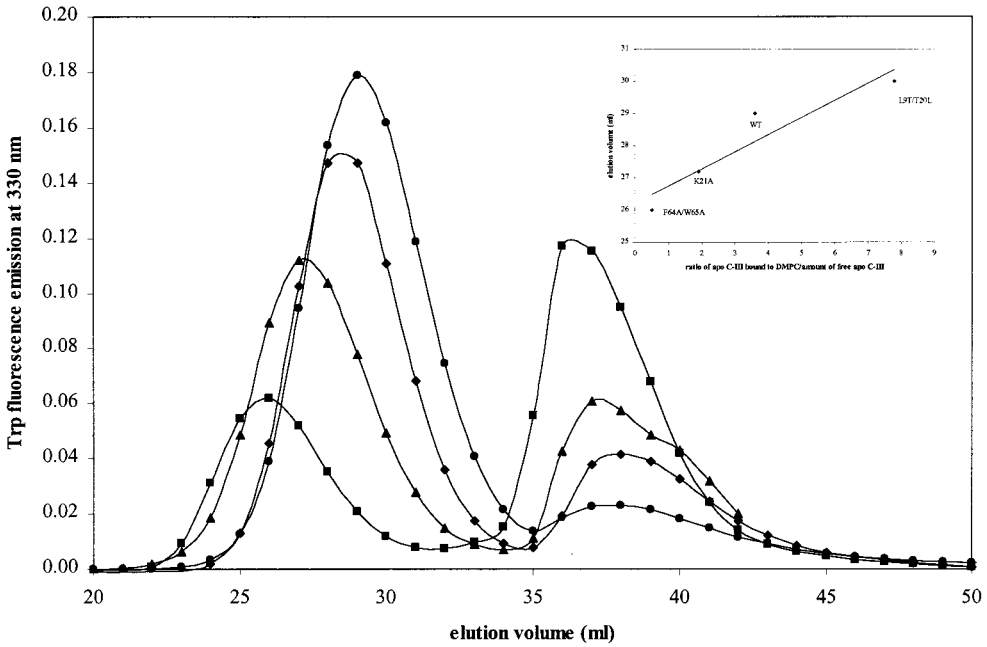

FIGURE 4: Gel filtration on a Superose 6 HR column of DMPC/apoC-III complexes with (◆) WT apoC-III, (▲) apoC-III-K21A, (■) apoC-III-F64A/W65A, and (●) apoC-III-L9T/T20L. Tryptophan fluorescence emission was measured at 330 nm as a function of the elution volume in milliliters. Inset: Regression line between size (elution volume in milliliters) and ratio of apoC-III bound to DMPC/amount of free as determined from the gel filtration elution profiles.

(Figure 4); the apoC-III protein in these fractions was monitored by measuring the Trp emission at 330 nm. In all the gel filtration runs, no free lipid could be detected which would typically elute within the void volume of the column (below an elution volume of 20 mL). All the apoC-III:DMPC complexes eluted as homogeneous peaks, although the amount of unbound apoC-III and the size of the discoidal complexes formed were quite different for each protein. The elution volume of the complexes varied from 26 mL (calculated Stokes radius 80 Å or 733 kDa) for the largest complex formed with the apoC-III-F64A/W65A variant to 29.5 mL (calculated Stokes radius 54 Å or 185 kDa) for the smallest complex formed with the apoC-III-L9T/T20L variant. The elution volumes of the DMPC complex of wild-type apoC-III and mutant apoC-III-K21A were 29 and 27.3 mL, respectively, corresponding to Stokes radii of 61 and 72 Å. The fraction eluting at 38 mL corresponds to unbound apoC-III, due to the small molecular mass of the protein, and is well separated from the protein:phospholipid complexes. Remarkably, however, for the different apoC-III proteins the shape and the maximum elution volume for the "lipid free" apo C-III vary slightly. The differences in elution behavior might represent partly lipidated apoC-III intermediates. Note that the heterogeneity in this fraction is highest for the poorest lipid binder, apoC-III-F64A/W65A. This variant was also associated with the highest amount of unbound/free apoC-III protein while apoC-III-L9T/T20L resulted in the lowest amount of the unbound/free protein among all the apoC-III variants, despite the fact that identical amounts of protein, lipid, and protein:lipid incubation ratios were used for the preparation of the complexes. A clear correlation between elution volume (i.e., Stokes radius) and the bound:free apoC-III ratio could be observed and is represented in the inset of Figure 4 ($r = 0.9$).

Physicochemical Characteristics of the Lipid-Free and Lipid-Bound ApoC-III Variants. The secondary structures of the apoC-III proteins and apoC-III/TFE mixtures were determined by CD measurements (Figure 5 and Table 2). All the apoC-III variants showed fairly random structure in buffer solution with typical minima around 200 nm. The propensity to form an α-helical structure was demonstrated by adding 50% TFE. The large increases in secondary structure are illustrated in Figure 5; in all spectra, the two typical minima were approximately 208 and 222 nm, and the single maximum at 190 nm was observed. These wavelengths are typical features of an α-helical structure. The spectra were deconvoluted according to the method described, and the results are summarized in Table 2. The increase in the α-helical content was most pronounced for the apoC-III-F64A/W65A variant (+54%), followed by apoC-III-K21A and apoC-III-L9T/T20L (+31%) and less pronounced for wild-type apoC-III (+25%) (Table 2), demonstrating the different abilities of each apoC-III variant to fold as an α-helix.

Table 2: Secondary Structure of ApoC-III Proteins Determined by CD in the Presence or Absence of 50% TFE

protein	α-helix (%)	β-sheet (%)	random coil (%)	Δ increase % α-helix
apoC-III wild type	20	41	39	
apoC-III-K21A	23	35	42	
apoC-III-F64A/W65A	20	45	35	
apoC-III-L9T/T20L + TFE 50%	20	41	39	
apoC-III wild type	45	29	26	25
apoC-III-K21A	54	24	22	31
apoC-III-F64A/W65A	74	16	10	54
apoC-III-L9T/T20L	51	26	23	31

The stability of the lipid-free apoC-III proteins and the apoC-III:DMPC complexes was estimated by following the decrease in their α-helical content measured by CD (molar ellipticity at 222 nm) after addition of increasing amounts of GdnHCl (Figure 6). The concentrations of GdnHCl at which 50% of the signal had decreased (the midpoints) are

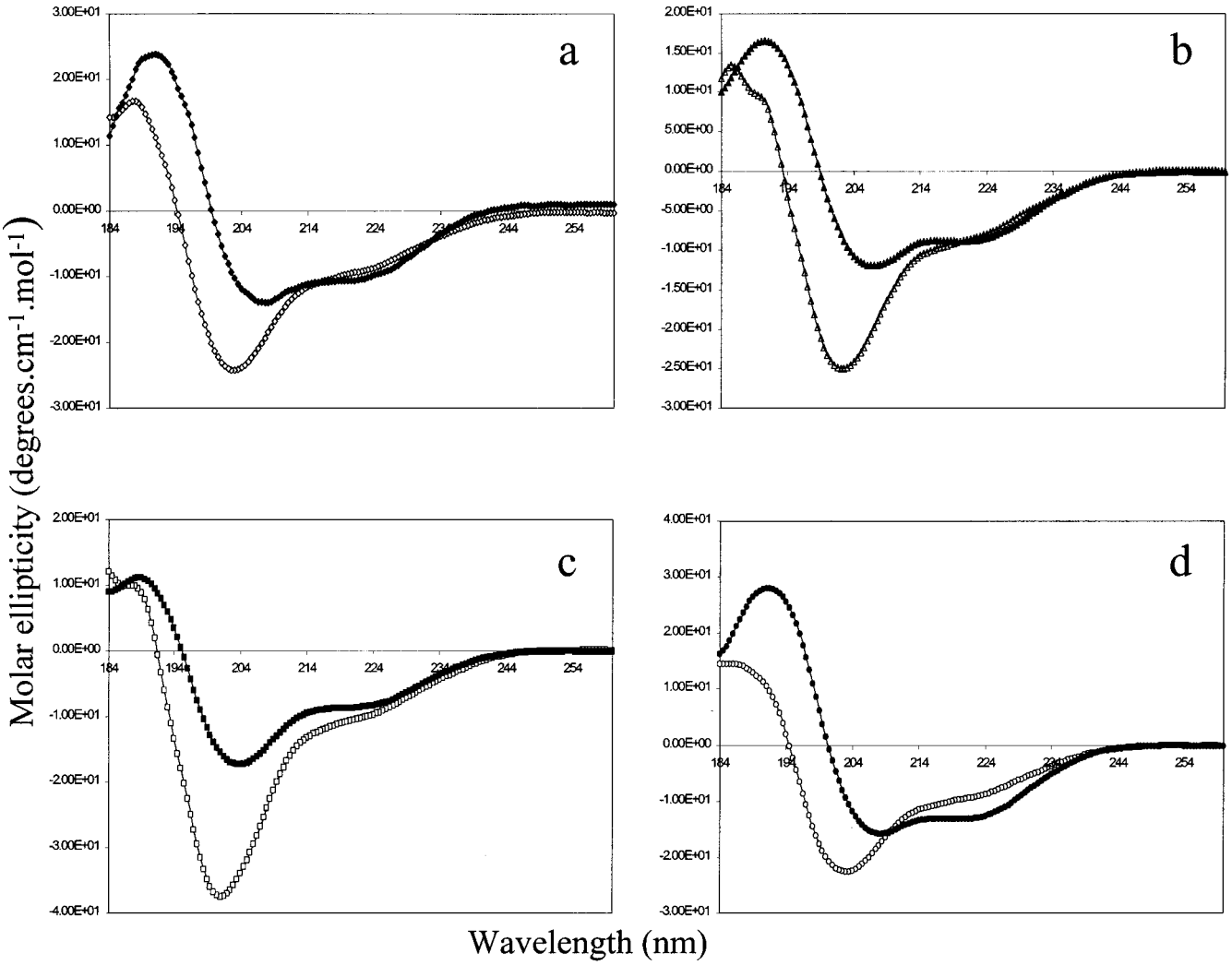

FIGURE 5: Circular dichroism spectra of apoC-III WT and mutant recombinant proteins in the presence (filled symbols) or in the absence (open symbols) of 50% TFE. Spectra recorded between 184 and 260 nm at 0.2 mg/mL protein, nine spectra averaged. (a) WT apoC-III; (b) apoC-III-K21A; (c) apoC-III-F64A/W65A; and (d) apoC-III-L9T/T20L.

Table 3: Physicochemical Characteristics of the Recombinant ApoC-III Variants

	Trp λ_{max} (nm), lipid-free	Trp λ_{max} (nm), lipid-bound	$\Delta\lambda_{max}$ [b]	$[GdnHCl]_{1/2}$ [a] (M), lipid-free protein	$[GdnHCl]_{1/2}$ [a] (M), apoC-III:DMPC
apoC-III wild type	343	333	10	1.3	3.0
apoC-III-K21A	343	333	10	1.5	2.4
apoC-III-F64A/W65A	343	333	10	1.8	2.0
apoC-III-L9T/T20L	343	331	12	1.0	3.4

[a] Concentration of GdnHCl (M) required to obtain 50% reduction in the CD signal measured at 222 nm as a measure of protein denaturation. [b] The "blue shift" in the Trp emission maximum.

summarized in Table 3. The midpoints of all the lipid-free apoC-III proteins (Figure 6A) were below 2 M; 1 M for apoC-III-L9T/T20L, 1.75 M for apoC-III-F64A/W65A, and 1.25 and 1.5 M for wild-type apoC-III and apoC-III-K21A, respectively. Once associated with DMPC (Figure 6B), the apoC-III proteins were stabilized and protected from denaturation by the phospholipid, resulting in a shift of each apoC-III:DMPC complex midpoint toward higher GdnHCl concentrations, as shown in the Table 3. The midpoint of the wild-type apoC-III:DMPC complex was 3 and 2.4 M for apoC-III-K21A:DMPC. ApoC-III-F64A/W65A:DMPC complex denatured more readily with the lowest midpoint of 2 M, suggesting a less stable lipid-associated complex, while the apoC-III-9L20T:DMPC complex showed the highest midpoint after DMPC binding, indicating the formation of the most stable apoC-III:DMPC complex. In addition, the fact that two-phase denaturation occurred for wild-type apoC-III:DMPC and apoC-III-L9T/T20L:DMPC complexes while one-phase denaturation occurred on apoC-III-F64A/W65A:DMPC and apoC-III-K21A:DMPC complexes is consistent with this result.

The maximum Trp emission wavelengths of the lipid-free and lipid-bound apoC-III proteins are also summarized in Table 3. The maximal wavelength of the Trp emission at 343 nm for all the lipid-free proteins shifted to 333 nm for the lipid-bound apoC-III proteins. In the case of the apoC-III-L9T/T20L, an even larger blue shift of 12 nm was observed. The observed blue shifts illustrate that the apoC-

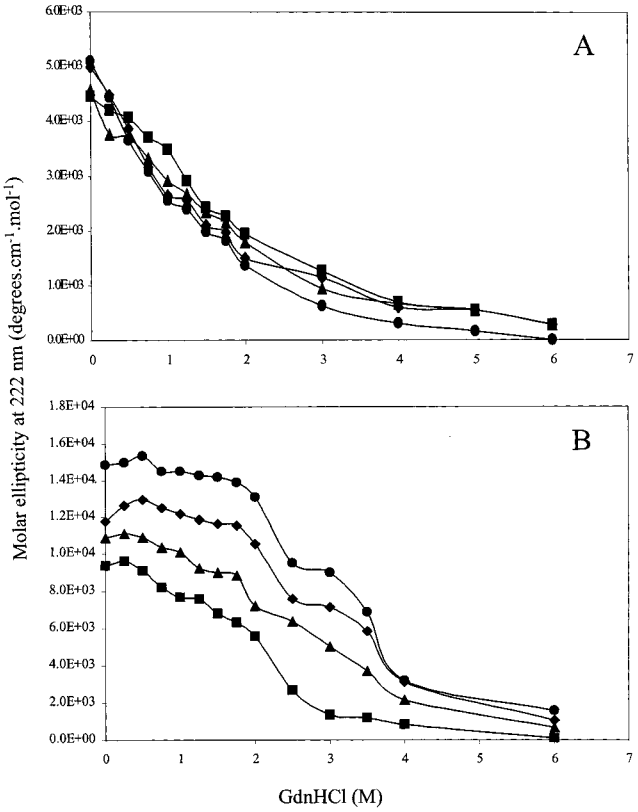

FIGURE 6: Denaturation of native (A) and DMPC−apoC-III complexes (B) monitored by measuring the decrease in molar ellipticity measured at 222 nm at increasing GdnHCl (M) concentrations in the incubation mixture with (◆) WT apoC-III, (▲) apoC-III-K21A, (■) apoC-III-F64A/W65A, and (●) apoC-III-L9T/T20L.

III tryptophans are buried in a more hydrophobic environment, due to the lipid binding.

Displacement of ApoE by ApoC-III Variants from Discoidal ApoE:DPPC Complexes. The capacity of apoC-III variants to displace apoE from the reconstituted apoE:DPPC complexes was followed by analyzing gel filtration profiles of apoE:DPPC:apoC-III mixtures (a) to check the integrity of the original apoE:DPPC complexes and (b) to identify the redistribution of apoE and apoC-III on the particles. The apoE:DPPC complex eluted at its original elution volume of 29 mL, and any displaced apoE or unbound apoC-III, not associated with the complex, eluted at higher elution volumes of 34 mL for apoE and 37 mL for apoC-III (data not shown). Western blotting was used to determine the distributions of both apoE and apoC-III in the fractions. All the apoC-III variants bound to the apoE:DPPC complex, while a fraction of the apoE was displaced from its original complex and could be detected at higher elution volumes. These results illustrate that apoE had been displaced by apoC-III from the complex, and that apoC-III had been incorporated into the apoE:DPPC complex. A more accurate quantification by analysis of the distribution of both apoC-III and apoE in these gel filtration runs was determined by measuring by ELISA the masses of both apoC-III and apoE in the individual fractions (Table 4).

From this table, it is clear that for all apoC-III proteins bound to the complex, for the apoC-III-F64A/W65A variant alone, this amount was reduced as compared with wild-type apoC-III. However, the amount of apoE displaced from the complex (Table 4) was quite different among the variants.

Table 4: Mass (μg) of ApoC-III Bound to or Mass of ApoE Displaced from ApoE:DPPC Complexes[a]

	apoC-III (μg) bound on complex	apoE (μg) displaced from complex
apoC-III wild type	62.2	6
apoC-III-K21A	65.3	10.2
apoC-III-F64A/W65A	35.0	0.1
apoC-III-L9T/T20L	46.2	21.9

[a] The mass of apoC-III or apoE was measured by ELISA in each fraction of the gel filtration run of the respective apoE:DPPC:apoC-III mixtures.

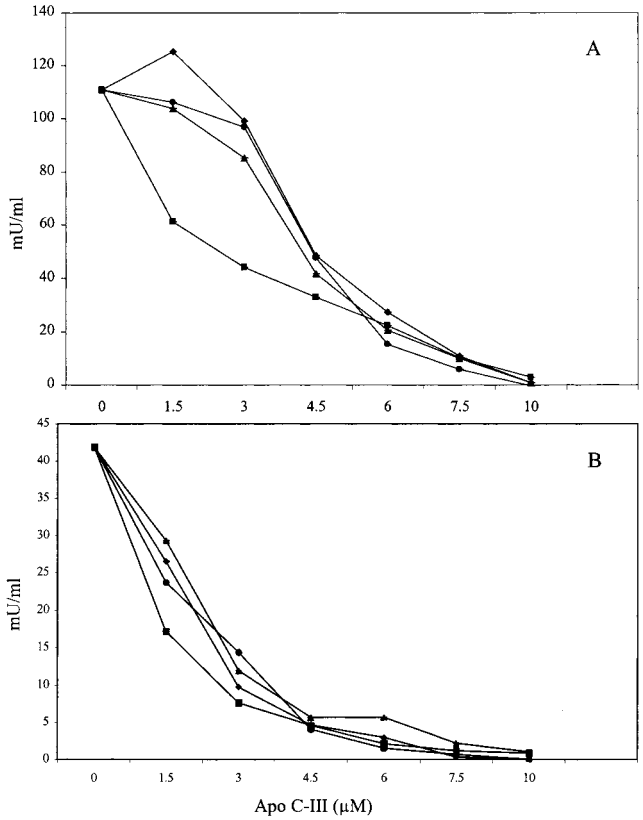

FIGURE 7: Inhibition of LPL by different recombinant apoC-III variants using Intralipid as substrate. Bovine LPL (15 ng) was incubated for 30 min at 25 °C in a total volume of 200 μL with ^{3}H-labeled Intralipid in the presence (A) and in the absence (B) of 40 ng of human apoC-II protein. (◆) WT apoC-III; (▲) apoC-III-K21A; (■) apoC-III-F64A/W65A; and (●) apoC-III-L9T/T20L. Each data point is the mean of triplicate samples. LPL activity is expressed as nanomoles of fatty acids per minute per milliliter.

While wild-type apoC-III and apoC-III-K21A displaced between 6 and 10 μg of apoE from the complex, this increase was much more pronounced for the apoC-III-L9T/T20L variant (22 μg) and very much reduced for the apoC-III-F64A/W65A variant (0.3 μg), suggesting that the lipid affinity of the apoC-III protein determined the ability to displace apoE from its complex.

LPL Inhibition by ApoC-III Variants. To identify the domains and residues of apoC-III that are responsible for LPL inhibition, the inhibitory effect of all the recombinant apoC-III variants was tested in the bovine LPL assay (Figure 7. Inhibition of the recombinant apoC-III was half that of the plasma human apoC-III in all cases (data not shown). All the recombinant apoC-III variants were able to inhibit LPL activity efficiently, both in the absence and in the presence of human apoC-II. However, in the presence of

apoC-II, the LPL inhibition was less pronounced at lower apoC-III concentrations (0−1.5 μM), with wild-type apoC-III showing an increase in LPL activity at these concentrations. From concentrations of 3 μM, the inhibition by all the apoC-III variants was well pronounced, and LPL activity was fully inhibited at apoC-III concentrations above 10 μM. In the absence of apoC-II, all the apoC-III variants showed effective inhibition at lower apoC-III concentrations. Comparing the I_{50} of each apoC-III variant, in the absence of apoC-II, the I_{50} of apoC-III-F64A/W65A was 1.3 μM while all the other apoC-III variants had a similar I_{50}, around 2 μM. In the presence of apoC-II, the I_{50} for apoC-III-F64A/W65A was 2 μM, and for the other apoC-III variants 4.4 μM.

DISCUSSION

ApoC-III plays a key role in TG-rich lipoprotein metabolism, but the structure/function relationship of apoC-III has not been fully elucidated. We have therefore generated several apoC-III variants according to protein modeling predictions, designed to alter specific amino acid residues implicated in lipid biding and LPL inhibition of apoC-III, to investigate the structure/function relationship of human apoC-III. Sequence analysis and secondary structure predictions applied to apoC-III indicate the existence of two helical domains that are rather amphipathic, as previously suggested (*11*, *27*). These segments were modeled, and mutants were designed to investigate further their role in the structure/function relationship of apoC-III. ApoC-III-K21A was designed to alter putative protein−protein binding properties in the N-terminus of apoC-III; apoC-III-L9T/T20L altered the angle of the tilted peptide located at residues 6−20 of apoC-III from 45° to 0°, and the apoC-III-F64A/W65A double mutation was designed to perturb the lipid binding properties of apoC-III by replacing two adjacent carboxyl-terminal aromatic amino acids with alanine.

Lipid Binding. Pownall and co-workers (*44*) have described that the rate of lipid−protein association was inversely correlated with the polypeptide molecular weight. In agreement with this, since apoC-III is a small protein, our DMPC clearing studies show a very efficient and fast clearing of the multilamellar DMPC solution.

Thrombin cleavage of apoC-III results in an N-terminal domain (residues 1−40) and a C-terminal domain (residues 41−79). Trieu et al. reported that the binding of apoC-III to surface phospholipid was mediated by the C-terminal helix between residues 50 and 62 (*45*). Indeed the association with DMPC indicated that the apoC-III-F64A/W65A showed severely diminished lipid binding properties, which confirms the original findings by Trieu et al. By analogy, it has been shown that the lipid binding domains in apoE and apoA-I are also localized in the C-terminus (*38*, *46*).

Sparrow et al. concluded that the N-terminus of apoC-III (residues 1−40) was not involved in binding to lipid (*11*). Our results suggest otherwise; since the mutant apoC-III-L9T/T20L showed significantly increased lipid binding properties compared to wild-type apoC-III, the contribution of the N-terminus to overall lipid binding may be important. Our results indicate that the change in orientation of the N-terminal helix influences the lipid binding properties of the whole protein and the overall stability of the protein: phospholipid complexes.

The size of the discoidal apoC-III:DMPC particles was dependent on the lipid binding properties of the variants. Whereas the WT apoC-III formed complexes with Stokes radii comparable to those reported by others (*47*), the size of the complexes formed with the poor lipid binder (apoC-III-F64A/W65A) was much larger than that of WT apoC-III particles, while the apoC-III mutant with enhanced lipid binding (apoC-III-L9T/T20L) formed disks with smaller radii as compared to WT. The relationship between size of discoidal complexes formed and lipid binding properties of apolipoprotein mutants was also observed in studies on apoA-I mutants (*46*).

A common observation is the increase in α-helical content of the apolipoprotein going from an aqueous solution to a lipid-bound state (*47*). Previous reports (*47*) show for apoC-III on average 26% α-helix in solution and 65−70% α-helix when lipid-bound. Careful analysis and deconvolution of our entire CD spectra (±50% TFE) showed a comparable increase in α-helicity in the presence of the helix-promoting solvent TFE for the WT and mutants K21A and L9T/T20L. In contrast, the double F64A/W65A mutant showed a larger increase in α-helical structure in TFE. This might be due to the fact that the mutation of those two bulky residues, located at the C-terminal extremity of the predicted second amphipathic helix, drastically improved the propensity of this segment to fold as an α-helix. Elimination of two consecutive bulky hydrophobic residues should favor α-helix formation. However, as a consequence of these mutations, the lipid binding affinity of this mutation was severely decreased, suggesting that these hydrophobic C-terminal residues in apoC-III have important functions in the initial interfacial recognition between the polypeptide and the phospholipid acyl chains during the initial phases of lipid binding.

In water, the maximum of Trp fluorescence emission for all apoC-III proteins tested was 343 nm, which is consistent with previous reports (*46*, *47*). These data also suggest that (a) the Trp residues in the recombinant apoC-III are fully exposed to water, (b) the recombinant apoC-III proteins are not in a highly aggregated state, and (c) the shift of the fluorescence maximum emission to lower wavelengths (blue shift) in the presence of lipids indicates shielding of the Trp from the water and replacement of the local Trp environment by lipid molecules. In the case of the apoC-III proteins, this shift was quite large (10 nm) and even larger (12 nm) for one of our mutants tested (L9T/T20L), suggesting an even deeper insertion of this mutant in the lipid phase. These observations are consistent with the higher lipid binding affinity of this mutant and suggest a tight association with the phospholipids for this particular mutant.

The [GdnHCl] at which both free and lipid-bound proteins denatured is comparable to the values reported for other apolipoproteins such as apoE and apoA-I (*38*). The difference in denaturation behavior between the WT and some of the mutants suggests differences in the overall stability of the protein folds. The WT, K21A, and L9T/T20L lipid-bound mutants denatured in a biphasic manner as reported for apoE (*38*), suggesting that the unfolding of the lipid-bound apoC-III might also occur through stable intermediates. The results for the L9T/T20L mutant suggest an overall higher stability when lipid-bound, due to its deeper insertion into the lipid phase as evidenced by the Trp emission behavior of this mutant. In contrast, the F64A/W65A mutant contains a high

percentage of α-helix; however, the monophasic denaturation pattern of this mutant suggests that the protein−lipid association is less tight and more prone to GdnHCl-induced denaturation.

The mechanism by which apoC-III influences plasma Tg levels has been the subject of debate. There is considerable evidence that this is due, in part, to the effects on apoE-mediated clearance of Tg-rich particles. Cross-breeding of apoC-III transgenic mice with apoE transgenic mice normalizes plasma Tg levels. From these studies, it was concluded that delayed clearance of VLDL Tg in the apoC-III over-expressors was due to the low amount of apoE relative to apoC-III on the VLDL particle Other studies suggest, however, that the hypertriglyceridemia in the apoC-III/apoE transgenic crosses is due to excess apoC-III on VLDL rather than apoE displacement (*14*). We chose to analyze the apoE displacement by apoC-III on discoidal apoE complexes because (a) these particles are more homogeneous than VLDL or HDL isolated from individual donors, (b) endogenous apoC-III would affect the experiments, and (c) apoC-III-deficient plasma was not available. Moreover, it is known that variable exchangeable pools of apoE are present in plasma VLDL and HDL (*15*). The displacement of apoE by apoC-III depends on the lipid binding affinity of the apoC-III, as reported previously for displacement of apoA-I by apoA-II (*40*). ApoC-III-L9T/T20L, the variant with the strongest lipid binding properties, replaced 31.2% of apoE from the apoE:DPPC complex (WT apoC-III displaced 17%), while only 8.4% of apoE was replaced by apoC-III-F64A/W65A, the variant with diminished lipid binding properties.

LPL Inhibition. The results obtained from the study by McConathy et al., examining the LPL inhibition by synthetic apoC-III peptides, suggested that the N-terminal domains of apoC-III, in particular the segments containing amino acids 1−7 and amino acids 17−25, are important in the modulation of LPL activity (*12*). In the current study, mutation of K21A and permutation of L9T/T20L in the N-terminus of apoC-III showed LPL inhibition comparable to recombinant wild-type apoC-III, suggesting that these changes do not affect LPL inhibition. These data therefore do not provide any further insight as to whether the N-terminus of apoC-III is involved in LPL inhibition, and additional mutations might be necessary to examine this. However, the fact that all the recombinant apoC-III variants inhibited LPL more efficiently than plasma apoC-III suggests that the *N*-glycosylation of plasma apoC-III may in fact modulate LPL inhibition.

ApoC-III-F64A/W65A, which bound least well to DMPC particles, displayed the most inhibitory effect on LPL, and this strongly suggests that LPL inhibition by apoC-III is unlikely to depend entirely on lipid binding leading to the displacement of apoC-II or LPL from the lipid substrate. Furthermore, the enhanced lipid binding of apoC-III-L9T/T20L did not appear to alter LPL inhibition, suggesting that these two functions are independent. The fact that apoC-III with altered lipid binding capacity can inhibit LPL activity is consistent with the notion that apoC-III inhibition of LPL lipolysis is due to protein:protein interactions rather than protein:lipid interactions (*48*). The involvement of the C-terminus of apoC-III in LPL inhibition supports the findings of Sparrow et al., who showed that the inhibitory effect of apoC-III could be localized to the C-terminal domain between residues 41 and 79 (*11*). This current study allows us to speculate on the mechanism of LPL inhibition by apoC-III. ApoC-III variants were able to inhibit LPL activity in the presence or absence of the LPL activator apoC-II, although with different I_{50}. In the presence of apoC-II, low concentrations of apoC-III inhibit less efficiently LPL, and in fact at low concentrations of wild-type apoC-III, LPL activity increased. Since apoC-III-F64A/W65A bound poorly to lipid, increased amounts of free apoC-III-F64A/W65A may directly interact with LPL. We therefore suggest that apoC-III inhibition of LPL may result from the balance of direct protein:protein interaction. Whether apoC-III interacts directly with apoC-II cannot be resolved by these results, and additional experiments would be needed to resolve this.

Taken together, these data identify that the hydrophobic residues F64 and W65 are crucial for the lipid binding properties of apoC-III and redistribution of the N-terminal helix of apoC-III (L9T/T20L) enhances the stability of the lipid-bound protein. Thus our structure/function relationship studies of wild type and mutant apoC-III suggest that the C-terminal hydrophobic residues in the sequence have important functions in the initiation of lipid binding, while redistribution of the hydrophobicity of the N-terminal helix improves the lipid binding and stability of the apoC-III polypeptide. This suggests that the N-terminal domain of apoC-III is necessary for the efficient functioning of WT apoC-III and/or normal lipoprotein metabolism. Indeed, this imperfect amphipathic domain could serve, for example, to balance apolipoprotein exchange. This is consistent with our results on the displacement of apoE from preformed complexes which is dependent on the lipid affinity of the apoC-III mutant tested. Our results further suggest that the inhibition of LPL activity by apoC-III is independent of the ability to bind lipids and by doing so to displace the LPL activator apoC-II, but may be due to direct protein:protein interactions with LPL and/or apoC-II. Further studies will be required to clarify these points.

REFERENCES

1. Shoulders, C. C., Harry, P. J., Lagrost, L., White, S. E., Shah, N. F., North, J. D., Gilligan, M., Gambert, P., and Ball, M. J. (1991) *Atherosclerosis 87*, 239.
2. Castelli, W. P. (1992) *Am. J. Cardiol. 70*, 3H.
3. Bainton, D., Miller, N. E., Bolton, C. H., Yarnell, J. W., Sweetnam, P. M., Baker, I. A., Lewis, B., and Elwood, P. C. (1992) *Br. Heart J. 68*, 60.
4. Koren, E., Corder, C., Mueller, G., Centurion, H., Hallum, G., Fesmire, J., McConathy, W. D., and Alaupovic, P. (1996) *Atherosclerosis 122*, 105.
5. Blankenhorn, D. H., Alaupovic, P., Wickham, E., Chin, H. P., and Azen, S. P. (1990) *Circulation 81*, 470.
6. Chivot, L., Mainard, F., Bigot, E., Bard, J. M., Auget, J. L., Madec, Y., and Fruchart, J. C. (1990) *Atherosclerosis 82*, 205.
7. Dolphin, P. J. (1992) in *Structure and Function of apolipoproteins* (Rosseneu, M., Ed.) pp 295−362, CRC Press, Ann Arbor.
8. Smith, L. C., and Pownall, H. J. (1984) in *Lipases*, p 263, Elsevier Science Publishers, Amsterdam.
9. Catapano, A. L., Lambert, D. A., Smith, L. C., Sparrow, J. T., and Gotto, A. M., Jr. (1996) *Chem. Phys. Lipids 127*, 205.
10. Lambert, D. A., Catapano, A. L., Smith, L. C., Sparrow, J. T., and Gotto, A. M., Jr. (1996) *Atherosclerosis 127*, 205.
11. Sparrow, J. T., Pownall, H. J., Hsu, F. J., Blumenthal, L. D., Culwell, A. R., and Gotto, A. M. (1977) *Biochemistry 16*, 5427.
12. McConathy, W. J., Gesquiere, J. C., Bass, H., Tartar, A., Fruchart, J. C., and Wang, C. S. (1992) *J. Lipid Res. 33*, 995.

13. Aalto Setala, K., Fisher, E. A., Chen, X., Chajek Shaul, T., Hayek, T., Zechner, R., Walsh, A., Ramakrishnan, R., Ginsberg, H. N., and Breslow, J. L. (1992) *J. Clin. Invest. 90*, 1889.
14. Ebara, T., Ramakrishnan, R., Steiner, G., and Shachter, N. S. (1997) *J. Clin. Invest. 99*, 2672.
15. Breyer, E. D., Le, N., Li, X., Matinson, D., and Brown, W. V. (1999) *J. Lipid Res. 40*, 1875.
16. Talmud, P. J. (1992) in *Structure and function of apolipoproteins* (Rosseneu, M., Ed.) pp 123−158, CRC Press, Ann Arbor.
17. Assmann, G., von Eckardstein, A., and Funke, H. (1992) in *Structure and function of apolipoproteins* (Rosseneu, M., Ed.) p 85122, CRC Press, Ann Arbor.
18. Ginsberg, H. N., Le, N. A., Goldberg, I. J., Gibson, J. C., Rubinstein, A., Wang Iverson, P., Norum, R., and Brown, W. V. (1986) *J. Clin. Invest. 78*, 1287.
19. Pullinger, C. R., Malloy, M. J., Shahidi, A. K., Ghassemzadeh, M., Duchateau, P., Villagomez, J., Allaart, J., and Kane, J. P. (1997) *J. Lipid Res. 38*, 1833.
20. Luttmann, S., von Eckardstein, A., Wei, W., Funke, H., Kohler, E., Mahley, R. W., and Assmann, G. (1994) *J. Lipid Res. 35*, 1431.
21. von Eckardstein, A., Holz, H., Sandkamp, M., Weng, W., Funke, H., and Assmann, G. (1991) *J. Clin. Invest. 87*, 1724.
22. Maeda, H., Hashimoto, R. K., Ogura, T., Hiraga, S., and Uzawa, H. (1987) *J. Lipid Res. 28*, 1405.
23. Roghani, A., and Zannis, V. I. (1988) *J. Biol. Chem. 263*, 17925.
24. Pillot, T., Barbier, A., Visvikis, A., Lozac'h, K., Rosseneu, M., Vandekerckhove, J., and Siest, G. (1996) *Protein Express. Purif. 7*, 407.
25. Gaboriaud, C., Bissery, V., Benchetrit, T., and Mornon, J. P. (1987) *FEBS Lett. 224*, 149.
26. Brasseur, R. (1991) *J. Biol. Chem. 266*, 16120.
27. Brasseur, R., Lins, L., Vanloo, B., Ruysschaert, J. M., and Rosseneu, M. (1992) *Proteins: Struct., Funct., Genet. 13*, 246.
28. Brasseur, R. (1990) in *Molecular description of biological membrane components by computer-aided conformational analysis* (Brasseur, R., Ed.) pp 203−219, CRC Press, Boca Raton, FL.
29. Geourjon, C., and Deleage, G. (1995) *Comput. Appl. Biosci. 11*, 681.
30. Rost, B., and Sander, C. (1993) *J. Mol. Biol. 232*, 584.
31. Rost and Sander, C. (1994) *Proteins: Struct., Funct., Genet. 19*, 55.
32. Frishman, D., and Argos, P. (1996) *Protein Eng. 9*, 133.
33. Garnier, J., Gibrat, J. F., and Robson, B. (1996) *Methods Enzymol. 266*, 540.
34. Deleage, G., and Roux, B. (1987) *Protein Eng. 1*, 289.
35. King, R. D., and Sternberg, M. J. (1996) *Protein Sci. 5*, 2298.
36. Levin, J. M., Robson, B., and Garnier, J. (1986) *FEBS Lett. 205*, 303.
37. Levin, J. M. (1997) *Protein Eng. 10*, 771.
38. De Pauw, M., Vanloo, B., Weisgraber, K., and Rosseneu, M. (1995) *Biochemistry 34*, 10953.
39. Vanloo, B., Morrison, J., Fidge, N., Lorent, G., Lins, L., Brasseur, R., Ruysschaert, J. M., Baert, J., and Rosseneu, M. (1991) *J. Lipid Res. 32*, 1253.
40. Labeur, C., Lambert, G., Van Cauteren, T., Duverger, N., Vanloo, B., Chambaz, J., Vandekerckhove, J., Castro, G., and Rosseneu, M. (1998) *Atherosclerosis 139*, 351.
41. Rosseneu, M. Y., and Labeur, C. (1990) *Curr. Opin. Lipidol. 1*, 508.
42. Bengtsson-Olivecrona, G., and Olivecrona, T. (1992) in *Lipoprotein analysis. A practical approach* (Converse, C. A., and Skinner, E. R., Eds.) pp 169−185, Oxford Unversity Press, New York.
43. Bengtsson Olivecrona, G., and Olivecrona, T. (1991) *Methods Enzymol. 197*, 345.
44. Pownall, H., Pao, Q., Hickson, D., Sparrow, J. T., Kusserow, S. K., and Massey, J. B. (1981) *Biochemistry 20*, 6630.
45. Trieu, V. N., and McConathy, W. J. (1995) *Biochem. Biophys. Res. Commun. 211*, 754.
46. Holvoet, P., Zhao, Z., Vanloo, B., Vos, R., Deridder, E., Dhoest, A., Taveirne, J., Brouwers, E., Demarsin, E., Engelborghs, Y., et al. (1995) *Biochemistry 34*, 13334.
47. Jonas, A. (1992) in *Structure and function of apolipoproteins* (Rosseneu, M., Ed.) pp 217−245, CRC Press, Ann Arbor.
48. Pownall, H. J., and Massey, J. B. (1986) *Methods Enzymol. 128*, 515.
49. Wang, C. S., McConathy, W. J., Kloer, H. U., and Alaupovic, P. (1985) *J. Clin. Invest. 75*, 384.

BI0009441